NANOFIBERS IN FILTER MEDIA

G. G. Chase and D. H. Reneker
The University of Akron

ABSTRACT

Current market and regulatory trends are pressing industries to improve filter media to capture particles in the submicron range. Common filtration wisdom tells us that to improve capture efficiency of submicron particles one must use smaller fibers. In this work, nanoscale fibers are added to larger glass fiber media. The modified media are tested and compared with conventional media. The results show that the use of the smaller fibers can improve the capture efficiency without the corresponding increase in pressure drop one would get by simply adding depth to the conventional media. This is an important application of nanofibers created via the electrospinning process. [This paper has been submitted to Chemical Engineering Science for publication].

INTRODUCTION

Recent market reports show the filtration market growing at a rate of about 35% per year, with strong growth in nonwovens. The total global filtration market is valued at about $3.25 billion USD with 41% sales in the Americas (22% for the USA), 35% in Europe, and 24% in Asia (Tirpak, 1999). The market for filtration equipment is estimated at $2.6 billion, with granular filters at $800 million in sales (Canning and Harrington, 1999). Some estimates of the future size of the industry range from $15 billion to an astounding $700 billion by the year 2020 (the latter based on the growth in biotechnology industries) (McIlvaine Company, 1999). Companies have significant interest in developing improved filter media to acquire larger shares of the market.

To develop improved filter media one requires an understanding of the controlling filtration mechanisms (Figure 1). The mechanisms of particle capture in a filter medium are cake formation, direct interception, inertial impaction, diffusional deposition, and gravitational capture (Brown, 1993). Cake formation occurs when particles are larger than a pore opening or when multiple particles bridge across a pore opening. Cake formation is analogous to screening, where large particles cannot pass through small openings between fibers, whereas, the other four mechanisms are single collector mechanisms due to the interactions between particles and single fibers of the filter medium.

Cake formation is most efficient with large particles and the single collector mechanisms are most efficient with very small particles. High capture efficiency occurs for very large particles and for very small particles; in between, in a range typically of about 100 to 800 nanometers, the efficiency is a minimum. This minimum efficiency corresponds to the most penetrating particle size.

The filtration mechanisms limit our options for improving the capture of particles in the most penetrating size range. But this size range is where some of the more innovative technologies are being developed.

One option is to use membranes for the separation of the particles from the fluid stream. Membranes have made astounding advances over the last 10 years. The disadvantage with membranes is that the high pressure drop required for a given flow rate requires such a large membrane area that the cost is often prohibitive.

Another option is to reduce fiber diameters in the filter media. Correlations show that capture efficiency tends to be inversely proportional to the fiber diameter (Brown, 1993). Direct interception capture efficiency is inversely proportional to the square of the fiber diameter,

$$E_{Direct} \propto \left(\frac{d_p}{d_f}\right)^2 \tag{1}$$

whereas efficiency due to inertial impaction in practical applications varies with the fiber diameter in a more complex relationship. For low Reynolds numbers the inertial efficiency varies with fiber diameter to a power between –3.8 and –2 and for high Reynolds numbers the inertial efficiency varies directly with the fiber diameter, as can be seen in the following relationships (Brown, 1993):

For Low Stoke's Number $$E_{Inertial} = E_{Direct} + (2\zeta)^{-2} J\, St \tag{2}$$

where ζ = Hydrodynamic Factor (constant)

$$St = \frac{d_p^2 \rho U}{18 \mu d_f} \quad \text{Stokes Number} \tag{3}$$

$$J = \left(29.6 - 28(1-\varepsilon)^{0.62}\right)\frac{d_p}{d_f} - 27.5\left(\frac{d_p}{d_f}\right)^{2.8} \tag{4}$$

For High Stoke's Number $$E_{Inertial} = 1 - \frac{c}{St} \tag{5}$$

where c is a constant that depends upon the flow field.

This contrasts with diffusional deposition for which the capture efficiency is inversely proportional to the fiber diameter to the 2/3 power (Brown, 1993):

$$E_{Diffusion} = 2.7\left(\frac{3\pi\mu d_p d_f}{C_n k_B T}\right)^{-2/3} \tag{6}$$

where C_n is the Cunningham Correction Factor due to aerodynamic slip, k_B is Boltzmann's constant, and T is the temperature.

In general for both direct interception and inertial impaction, when the particle diameter decreases the efficiency decreases. To improve the efficiency the fiber diameter also must decrease. For droplets in the 100 to 500 nanometer range, all three of these mechanism can be important. Equations (1) –(6) show the capture efficiency to be sensitive to the fiber diameter. Filter media enhanced by the incorporation of smaller fibers are a promising area for investigation.

POLYMER NANOFIBERS

Recent developments in electrospinning make it possible to produce, from many kinds of polymers, laboratory quantities of fibers with diameters in the range of 1 to 1000 nanometers (Reneker and Chun 1996). The photograph in Figure 2 shows Nomex™ nanofibers (approximately 200 nm in diameter) mixed with larger 5 to 10 um diameter glass fibers. Nomex is a tradename of the E.I du Pont de Nemours Company and stands for MPD-I (meta-aramid, poly (meta-phyneleneisophthalamide)). Nanofibers have a higher surface area to mass ratio compared to conventional fibers, which is advantageous. Other methods, such as meltblowing (John and Mcculloch, 2000) and fibrillation (Robeson *et.al.*, 1994; Robeson *et.al.*, 1992), are also used for producing submicron fibers. Electrospinning is applied in this work.

The electrospinning process is robust and fairly simple. The equipment for the laboratory scale apparatus consists of a pipette to hold the polymer, two electrodes, and an adjustable high voltage D.C. power supply, as shown in Figure 3. Key features of the electrospinning process are:

- A suitable solvent must be available for dissolving the polymer.
- The solvent must have a high enough vapor pressure that it evaporates quickly enough for the fiber to maintain its shape (and not to contract into droplets or break) by the time the fiber lands upon the receiving ground surface. Yet, the solvent must not evaporate so quickly that the fiber hardens before it is elongated so that diameters in the nanometer range are achieved.
- The viscosity and surface tension of the solvent must not be so large that they prevent the jet from forming, but they must not be so low that the polymer solution in the pipette drains freely under gravity.
- Typically, 20,000 volts are applied to overcome the viscosity and surface tension of the polymer solution to form and sustain the polymer jet from the pipette. The electrical current required is small, on the order of a few microamperes, so a limit of 100 microamperes is both convenient and safe.
- The gap distance between the pipette and the grounded surface is set to such a distance that the applied voltage difference is strong enough to drive the polymer jet, not so small that sparks jump between the electrodes, yet long enough that the solvent can evaporate in time for the fibers to form.

The electrospinning process has a number of competing forces that cause the fibers to elongate and stretch until they are in the nanometer diameter range (1 to 1000 nm). Evidence from high speed camera images shows that the jet predominately remains as one fiber. The current theory on process is that electrical charges are induced on and carried with the polymer jet due to the applied voltage. These charges are strongly repelled by each other, but are held in place for a time due to their axial alignment (see Figure 4).

The force in the transverse direction causes the fiber to stretch and elongate in that direction. The elongated fiber stabilizes momentarily, until another misalignment causes further stretching and elongation. Each stretching event causes the diameter of the fiber to decrease, as required by the mass continuity. The imbalanced force in the transverse direction causes the fiber to buckle and produces a bend in the polymer fiber. Subsequent stretches produces smaller bends in the fiber, as shown in Figure 5. After about 8 to 10 stretches the fiber diameter is in the nanometer range. A typical segment of the jet, as it leaves the pipette, is elongated by a factor of 10^5 when the jet dries into a solid fiber. A segment 10 microns long becomes a meter long.

The stretching and bending processes occur over the electrode gap distance of about 10 to 20 centimeters. The fibers move towards the receiving ground surface in what appears to be a conical shape. The appearance of a cone of fibers is due to the light reflecting off of the bends in the fiber. The fiber typically collects on a flat grounded surface in a circular pattern.

In experiments with filter media about 0.07 grams of fiber were spun from a single pipette in about 20 minutes. Compared to other fiber production processes this is a small mass rate (0.21 grams per hour). If we consider that the MPD-1 fiber has an average diameter of about 150 nm we can calculate its length.

$$(0.07grams)x\left(\frac{cm^3}{1.05grams}\right)x\left(\frac{m^3}{10^6cm^3}\right)x\left(\frac{4}{\pi(150nm)^2}\right)x\left(\frac{10^9nm}{m}\right)^2x\left(\frac{km}{1000m}\right)=3772km$$

Being produced in 20 minutes, this equates to an astounding fiber production rate of 11,317 km/hr with a correspondingly high rate of production of surface area!

The 11,000 km/hr rate of fiber production is the rate that would be obtained if some mechanism were available by which the fiber could be drawn out in a continuous line. Achieving such rates would require a large increase in kinetic energy, which is avoided by the coiled path of the actual jet. This rate however is impractical as it exceeds the speed of sound in solids. When the fiber elongates in the electrospinning process the bends and elongations occur in multiple directions over short distances hence the elongational velocity is not all in the same direction. On a mass inertial scale the effective velocity of the jet from the pipette to the grounded surface is only on the order of a few meters per second, a velocity much lower than that required to produce straight fiber at a comparable elongation rate.

The long lengths of the nanofiber can produce large surface areas that are useful in applications such as filtration. Figure 6 shows a log-log plot of how the specific surface area (m^2/g) varies with the diameter of the fiber from polymers of density of 1 gram per cubic centimeter.

Different polymers and solvents produce fibers of different sizes. The MPD-I fiber is among the smaller diameter nanofibers that are produced by electrospinning. Other polymers that have been electrospun at The University of Akron include nylon, acrylonytrile, and Ultem 1000 (a trademark of the GE Corporation). A list of polymers and solvents are given in Table 1.

Polymer nanofibers have a number of uses besides filter media. Nanofibers can be used in textiles for water repellency, as sorbant materials, as fibers for reinforcements in composite materials, supports for enzymes or catalysts that can promote chemical reactions, a support structure for growth of biological cells, pesticide and agricultural applications, components of nanoscale machines, matrices for molecular mechanisms, and as fabric for solar sails to transport cargo between planets.

COALESCENCE FILTRATION

The particular application of polymer nanofibers considered here is the coalescence of liquid droplets from a stream of gas. Coalescing filters are used throughout industry to separate small liquid droplets from gas streams or from another liquid phase. A number of factors influence the efficiency and economics of the separation. In general, droplets in a range of about 0.1 to 1 micron in size are the most difficult to remove.

Unlike other filter media whose primary purpose is to stop the particles from moving with the fluid stream, the coalescing filter media have the additional requirements of making the drops coalesce together into larger drops and of providing a means for the larger drops to drain out of the medium (Figure 7). In operations such as gas compression, the collected liquid is typically an expensive synthetic oil used in the compressor as a coolant, sealant, and lubricant. Coalescence filtration is used to recover and recycle the oil back to the compressor. Recovering ever smaller droplets also reduces airborne emissions in many processes helps to comply with environmental regulations.

The success of a coalescer filter depends upon the structure of the filter media. As in most filters, the filter medium controls whether the particles are captured in depth, collected on the surface, or passed through. The interaction between the medium and the incoming fluid determines both the pressure drop and separation efficiency.

There are many different types of filter media (woven fabric, nonwoven, sintered metal, foam, membranes, felts, paper, and ceramics) (Purchas, 1981). The design and construction of practical filter media are largely an art, and recipes are guarded trade secrets. As a result, the structure of the filter medium receives comparatively little attention in literature (Brown, 1993).

Filtration is a process that operates on many scales. Channels, structural elements and capture surfaces of a filter must be matched to the scale of the particles or droplets that are to be captured in the filter. Polymer nanofibers, made in our laboratory, provide a flexible and adjustable system for optimizing the scale of the filter structure to capture particles in the size range which has the highest probability for passing through the filter.

There are a number of mechanisms that control the coalescence process. Filtration capture mechanisms (described previously) control the rate at which drops are captured within the filter media. The filter media act to slow down the movement of the drops to cause the drops to collide. When the force and duration of the collisions are sufficient to overcome the surface tension the drops coalesce to form larger drops.

Microscopic observation of the coalescence process shows that most of the drops visible to the microscope (20 to 200 micron size range) are captured on the fibers (Chokdeepanich and Chase, 2000). . When the captured drops form beads on the fiber that are of large enough to see with an optical microscope, the growth of the beads is rapid. When the beads on the fiber become large enough to touch , the size of the beads no longer increase. Instead, the oil flows along the fiber toward a collection point. Figure 8 shows a smaller drop migrating along a fiber toward a larger drop and subsequently coalesces with the larger fiber over a period of several seconds.

The mechanisms controlling the movement and coalescence of drops on fibers are not well understood, though wettability and surface tension are known to be important factors. Highly wetting fiber surfaces tend to hold onto the drops by spreading the drops over the surface. A nonwetting surface does not hold onto the drops long enough for the beads to grow to a large size. As shown in Figure 9, the optimum conditions are somewhere in between the highly wetting and the nonwetting surfaces.

Several parameters, including pressure drop and capture efficiency, characterize the performance of filter media. It is convenient to have one parameter that accounts for multiple effects. Brown [1993] recommends using the quality factor, QF, defined by

$$QF = \frac{-\ln\left(C_{out}/C_{in}\right)}{\Delta P} \tag{7}$$

where $\left(C_{out}/C_{in}\right)$ is the penetration defined as the ratio of the concentration of particles passing through the filter to the or concentration of particles entering the filter, and ΔP is the pressure drop. The nature of capture efficiency is such that if you double the thickness of a filter medium the penetration decreases by the square of the thickness, hence the logarithm of the penetration is proportional to the thickness. On the other hand, the pressure drop is directly proportional to the filter thickness. Hence the quality factor is independent of the thickness of the medium and provides a means of direct comparison between various media.

EXPERIMENTAL DESCRIPTION

Coalescence experiments were run to measure the pressure drop and penetration while controlling the feed concentration and the flow rate through the filter medium on the apparatus diagrammed in Figure 10. Compressed air was preconditioned by drying and filtering. Part of the compressed air passed through a Laskin Nozzle (Air Techniques International) to generate the droplets while the rest of the air passed through a heater to heat the air to the desired operating temperature.

The heated air was mixed with the concentrate from the nozzle and was passed through the test medium, through a flow control valve, and through a flow meter. The temperature was measured a short distance upstream from the filter medium. A photometer that measures light attenuation due to the presence of particles in the air stream, via a calibration curve, was used to measure the upstream and down stream particle concentrations. A pressure gauge measured the pressure drop across the filter medium. Drain ports were provided for draining the collected oil from the test medium.

The temperature and humidity were controlled in the experiments. The applied pressure and flow rate were adjusted to the desired operating conditions. The pressure drop and flow rate were used to calculate the permeability of the medium. The pressure drop and particle concentrations in the gas stream entering and leaving the filter were used to determine the quality factor.

CONSTRUCTION OF FILTER MEDIA

To prepare a filter medium made of glass fiber and water based binder, 2 grams of glass fiber were mixed in 4 to 6 liters of water. A binder, 8ml of Carboset 560™ supplied by BF Goodrich, was added to the mixture. Sulfuric acid was added to the mixture to adjust the pH of the slurry to 2.5. The low pH helped to disperse the glass fibers. The slurry was stirred continuously to keep the glass fibers in suspension. Once the slurry was uniformly mixed, it was allowed to set for 24 hours while the binder in solution came to equilibrium with that on the glass fibers.

After 24 hours, the slurry was again stirred to a uniform suspension. The slurry was next pulled into a mold with a porous bottom by a vacuum. The other end of the mold was connected to an evacuated tank, which was in turn connected to the vacuum pump to supply the vacuum to the system. The vacuum pump maintained a pressure of about 500 mm of mercury. The tank captureed the acidic liquid during the vacuum forming process. After the medium was completely formed, it was removed from the mold and dried and cured in an oven at 150 C for 2 hours. The binder hardened during the curing step and the filter medium was ready for testing.

To make media with nanofibers, the nanofibers were added to the slurry mixture prior to vacuum forming. The slurry was well mixed to distribute the nanofibers throughout the medium. Scanning Electron Microscopy and optical microscope images, such as shown in Figure 2, confirmed the mixing of the nanofibers with the glass fibers throughout the medium.

EXPERIMENTAL RESULTS AND DISCUSSION

Effects of variables such as temperature, humidity, and flow rate were investigated. The results reported here are on the effects of adding nanofibers to the filter media with all other variables held constant. The diameters of the glass fibers and the polymer nanofibers used in the experiments are listed in Table 2 with their calculated surface areas per gram of fiber.

As an example, all of the filter media were made with 2 grams of glass fibers which amounts to 0.91 m^2 of surface area. The addition of 0.07 grams of nylon nanofibers added 1.0 m^2 of fiber surface area to the medium. This resulted in a medium with fiber surface area that is 52% nanofiber.

Figure 11 shows the pressure drop and Figure 12 shows the concentration data that are typical of the data obtained from experiments. For repetition of the experiments, four different media samples were tested. The samples were made the same way with 2 grams of glass fiber, 2 grams of Carboset 560™ binder, and 0.07 grams of nylon nanofiber. The data show the pressure drop started out at the value obtained for a clean filter medium with zero loading of oil. Over time the oil fills some of the pore spaces in the media and the pressure drop increased until it reached a steady state value. Similarly, the oil concentration in the outlet air started at zero and increased to a steady state value. The experimental results show that the steady state was reached after about 150 minutes and that the steady state values of pressure drop and outlet concentration were in reasonable agreement between the samples.

Using concentration and pressure drop data the quality factor in Eq. (7) can be calculated. In each experiment the droplet concentration upstream is 550 ppm. The most interesting results present themselves

when we plot the Relative Quality Factor (quality factor of glass and nanofiber medium divided by quality factor of medium of glass fiber only medium) versus the surface area fraction made up of nanofibers. Figure 13 shows the data from a number of experiments with media of glass fiber only and media with varying concentrations of nanofibers made of Nylon, MPD-I, PAN, or Ultem 1000.

Three experiments were run to determine the Quality Factor for Glass Fiber only. Two of the experiments yielded essentially the same Quality Factor of 1.652 PSI^{-1} while the third experiment gave a value of 1.900 PSI^{-1}. The former value was used to calculate the relative quality factors and the latter plotted in Figure 13 indicates the relative uncertainty in the data.

There are a number of mechanisms simultaneously affecting the filter medium performance. Figure 13 indicates that the nanofibers may not have significant influence on the performance of the medium when the nanofibers contribute to less than about 25% of the surface area of fibers. When the nanofibers contribute to more than 25% of the surface area they have a more significant affect on the performance. The best performance occurred with a mixture of 0.02 grams of Nylon 6 with 0.05 grams of MPD-I nanofibers.

One possible explanation for this behavior is that when the nanofiber provides less than 25% of the surface area, the glass fibers dominate the function of the filter. When the concentration of nanofibers is small there may be open pores and channels through which the fluid may bypass the nanofibers. When the amount of surface area provided by the nanofiber exceeds 25% there is a sufficient amount of nanofiber present to fill all of the pores between the glass fibers. Hence the media with larger amounts of nanofiber show higher capture efficiency without the corresponding increase in pressure drop. Another possible explanation is the surface properties of the nanofibers affect the capture mechanisms but only when their surface area exceeds 25% of the total area. Further work is needed to determine the controlling mechanisms.

The addition of conventional MPD-I (CMPD-I) fibers to the glass fibers causeed a decrease in the performance of the media as shown in Figure 13. The CMPD-I fibers do not contribute significantly to the total surface area but their presence seems to degrade the performance of the filter, as shown by the relative quality factors less than unity. Determining the cause for this requires additional experiments. We expect that the surface properties of the CMPD-I to be the similar to the surface properties of the MPD-I nanofibers, but that the nanofibers have much more surface area per unit mass. This suggests that the improved performance with the MPD-I nanofibers is more do to fiber filling the pore spaces than it is due to the surface properties of the MPD-I.

The data does not tell which of the filtration mechanisms (interception, inertial impaction, gravity, or diffusional interception) dominates the filter medium performance. The data do show that the addition of nanofibers has a significant and favorable effect on the performance of the glass fiber media.

CONCLUSIONS

This paper describes experiments done to evaluate performance of filter media enhanced with nanofibers. Experiments were conducted with several different polymers and with varying concentrations of nanofiber. The data show that there was a direct correlation between performance and the amount of nanofiber added to the media. A small mass of nanofiber added significantly to the surface area of the media. When the nanofibers contributed more than 25% of the surface area, then the filter medium performance improved significantly.

ACKNOWLEDGEMENTS

The AirMaze Corporation, Ahlstrom Filtration Inc., Donaldson Company, Filtrauto, Hankison International, J.C.Binzer Company, Parker Hannifin Finite Division and the National Science Foundation GRANT CTS-9900949 are acknowledged for the financial support of this research.

NOTATION

C_n	Correction factor for hydrodynamic slip, [-].
d_f, d_p	Fiber and particle diameters, [m].

$E_{Direct}, E_{Inertial}, E_{Diffusion}$	Filter media capture efficiencies due to mechanisms of direct interception, inertial impaction, and diffusional deposition, respectively, [-].
J	Function calculated via Eq.(4)
k_B	Boltzmann's constant
T	Temperature, [C].
U	Gas velocity
ζ	Hydrodynamic factor, [-].
ρ	Gas density, [kg/m^3].
μ	Viscosity of the gas, [kg/m/s].

REFERENCES

Brown, R.C., 1993, *Air Filtration*, Pergamon Press, Oxford.

Canning, K.,. Harrington, K. 1999 "News: Liquid Macrofiltration market to hit $3.7 billion in 2003," *Pollution Engineering*, 31(13), December 1999, (www.pollutionengineering.com).

Chokdeepanich, S. and Chase, G.G., 2000 "Microscopic Observatin of Droplet Coalescence in a Fiber Matrix," *Advances in Filtration and Separation Technology*, Volume 14, N. Bugli, W. Chen, and S. Reynolds eds., American Filtration and Separations Society, Northport, AL, 851-856.

John, W., Mcculloch, G., 2000 "Ultrafine to nanofine fibers via spun melt processes,", *Advances in Filtration and Separation Technology,* Volume 14, American Filtration and Separations Society, Northport, AL.

McIlvaine Company, 1999 *Clear Solutions*, No. 88, World Filtration Media Market, October 1999 (www.mcilvainecompany.com).

Purchas, D.B., , 1981Solid-Liquid Separation Technology, Uplands Press, Croydon, Great Britain.

Reneker, D.H. and I. Chun, , 1996 "Nanometre diameter fibers of polymer, produced by electrospinning," *Nanotechnology*, 7, 216-223.

Robeson, L.M., Axelrod, R.J., Vratsanos, M.S., and Kittek, M.R , 1994 "Microfiber Formation: Immiscible Polymer Blends Involving Thermoplastic Poly(vinyl alcohol) as an Extractable Matrix," *J Applied Polymer Science*, 52, 1837-1846.

Robeson, L.M., Axelrod, R.J., Kuphal ,J.A., and Pickering, T.L., 1992 "Process for the Prodcution of Ultra-Fine Polymeric Fibers," US Patent 5,164,132, November 17.

Tirpak, C.M., 1999 "Filtering out Trends in the Filtration Market," *Nonwovens Industry*, 30 (11), 42.

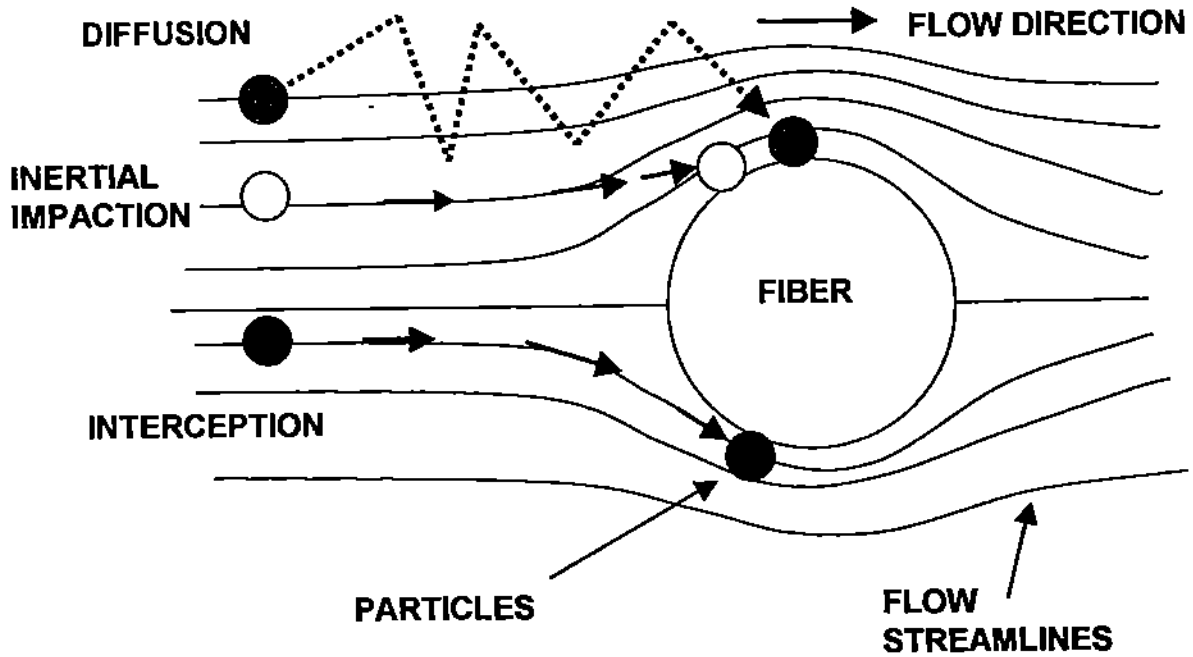

Figure 1. Filtration mechanisms. Particles following the flow streamlines are captured by direct interception. Large or dense particles can deviate from the streamlines due to their inertia and collide with fibers in their path. Small and low density particles are effected by Brownian motion that causes particles to diffuse to a fiber surface.

Figure 2 SEM image of nanofibers on larger glass fibers. The nanofibers are made of Nomex™ (tradename of fibers made by the DuPont Company) otherwise known as MPD-I (meta-aramid, poly (meta-phyneleneisophthalamide)).

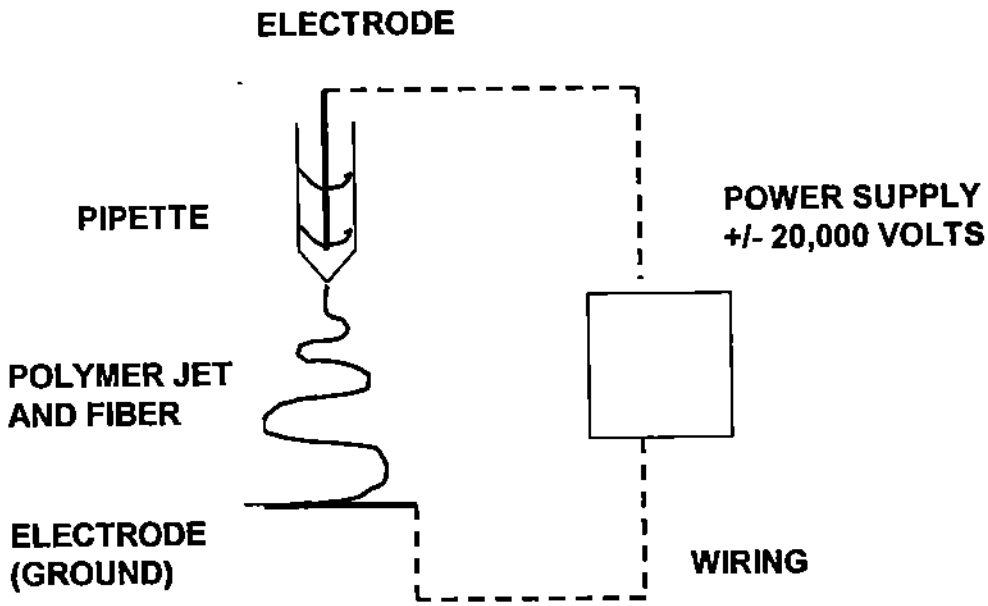

Figure 3. Sketch of the Electrospinning Process.

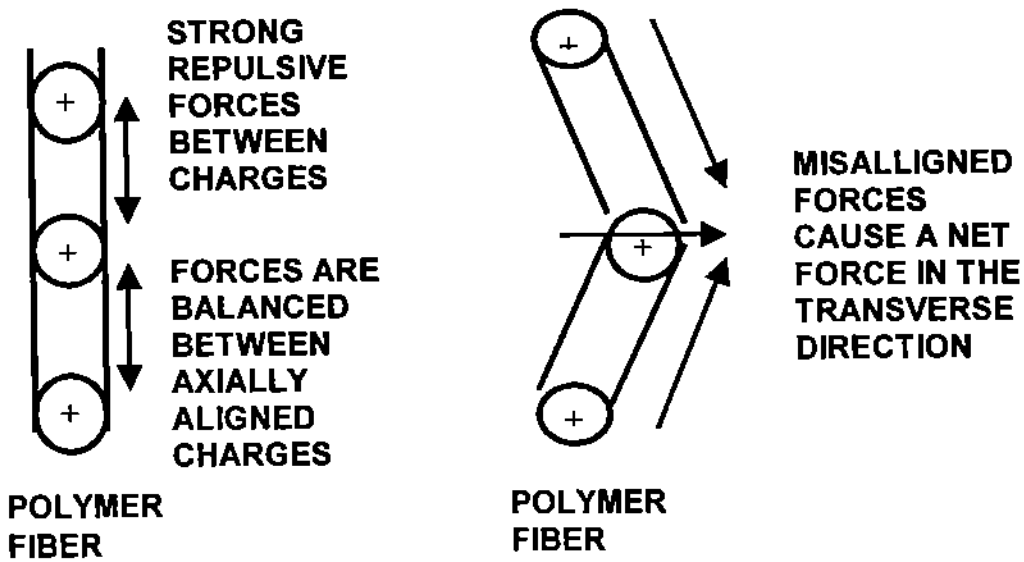

Figure 4. Electrical charge in the polymer jet causes the jet to elongate. The charges are in a pseudo-stable position as long as they are axially aligned. When molecular vibrations are sufficient to cause misalignment, the strong repulsive force causes a net force in the transverse direction. The transverse force causes a buckling of the fiber. The imbalanced forces also cause the fiber jet to elongate.

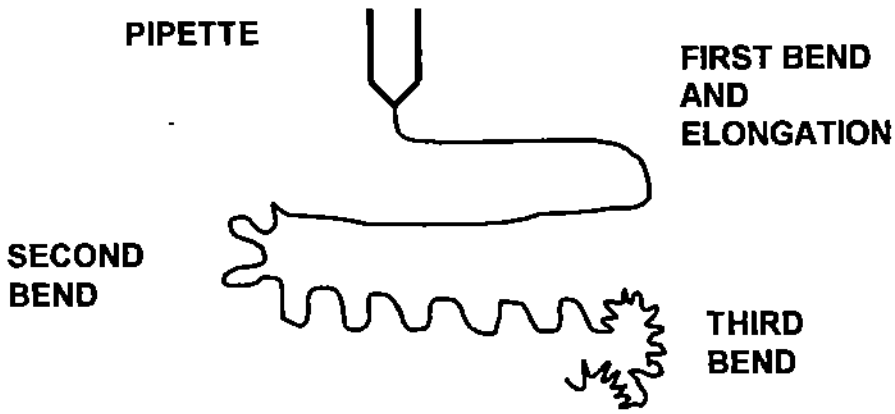

Figure 5. Each stretch and elongation of the polymer fiber causes the fiber to bend. This is a result of the net velocity of the fiber being less than the stretch and elongation velocity.

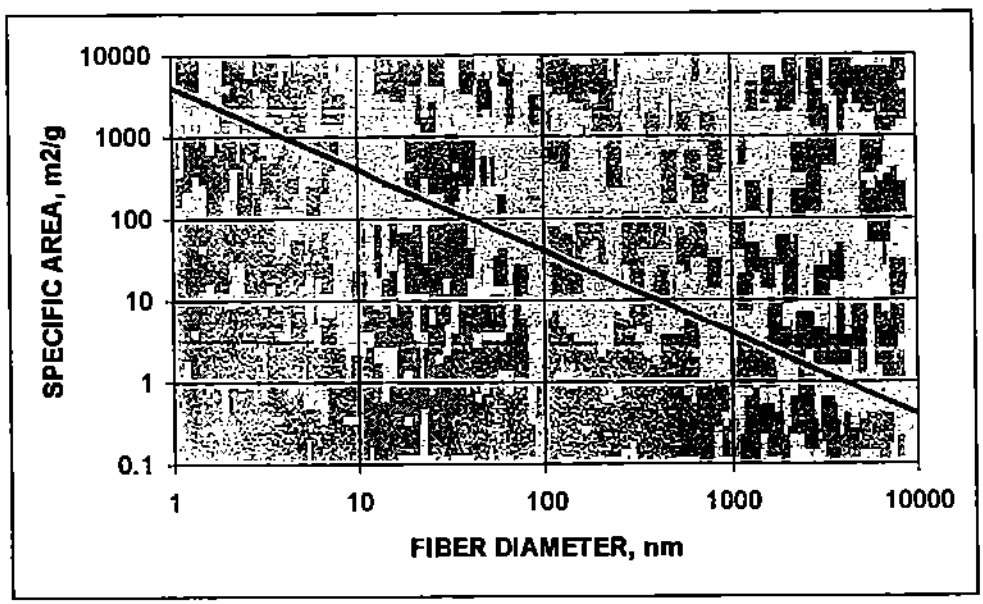

Figure 6. Plot of specific surface area versus fiber diameter for fibers with a mass density of 1 g/cm^3.

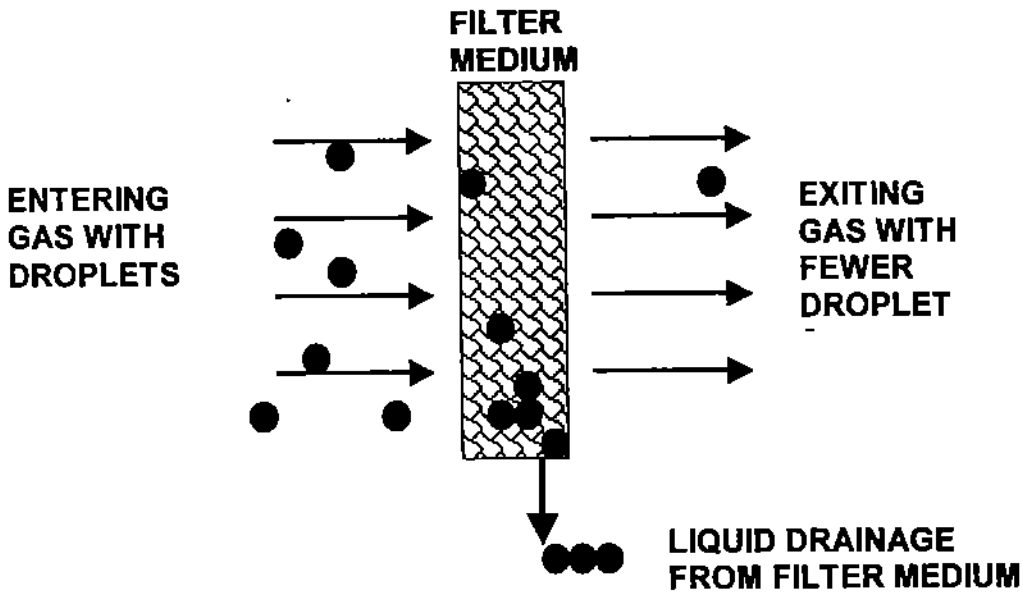

Figure 7. Coalescence filtration removes drops from the flow stream and drains the drops from the filter.

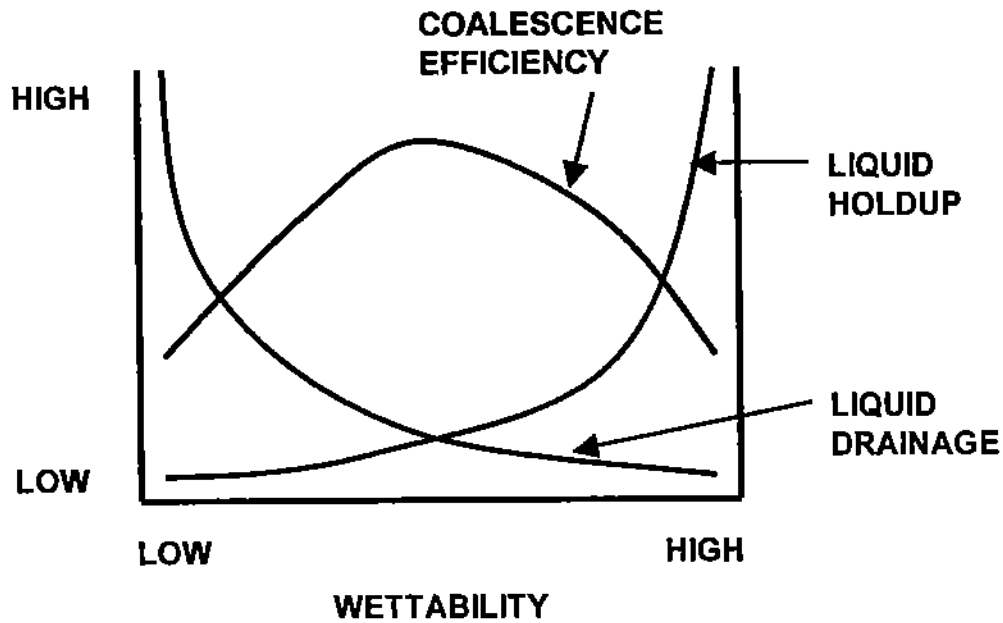

Figure 9. Highly wetting surfaces tend to hold large amounts of liquid. Nonwetting surfaces drain quickly and do not hold liquid drops. In terms of coalescer efficiency, the optimum surface material lies somewhere in-between the extremes.

0 SECONDS

15 SECONDS

30 SECONDS

Figure 8. Microscope photos of propylene glycol oil drops on glass fibers. In the top photograph, a large and a small drop are observed near each other on a fiber. In the subsequent photographs the smaller drop migrates towards the larger drop and the two drops coalesce. The photos cover a 30 second time duration. The scale in the lower right hand corner indicates 50 microns.

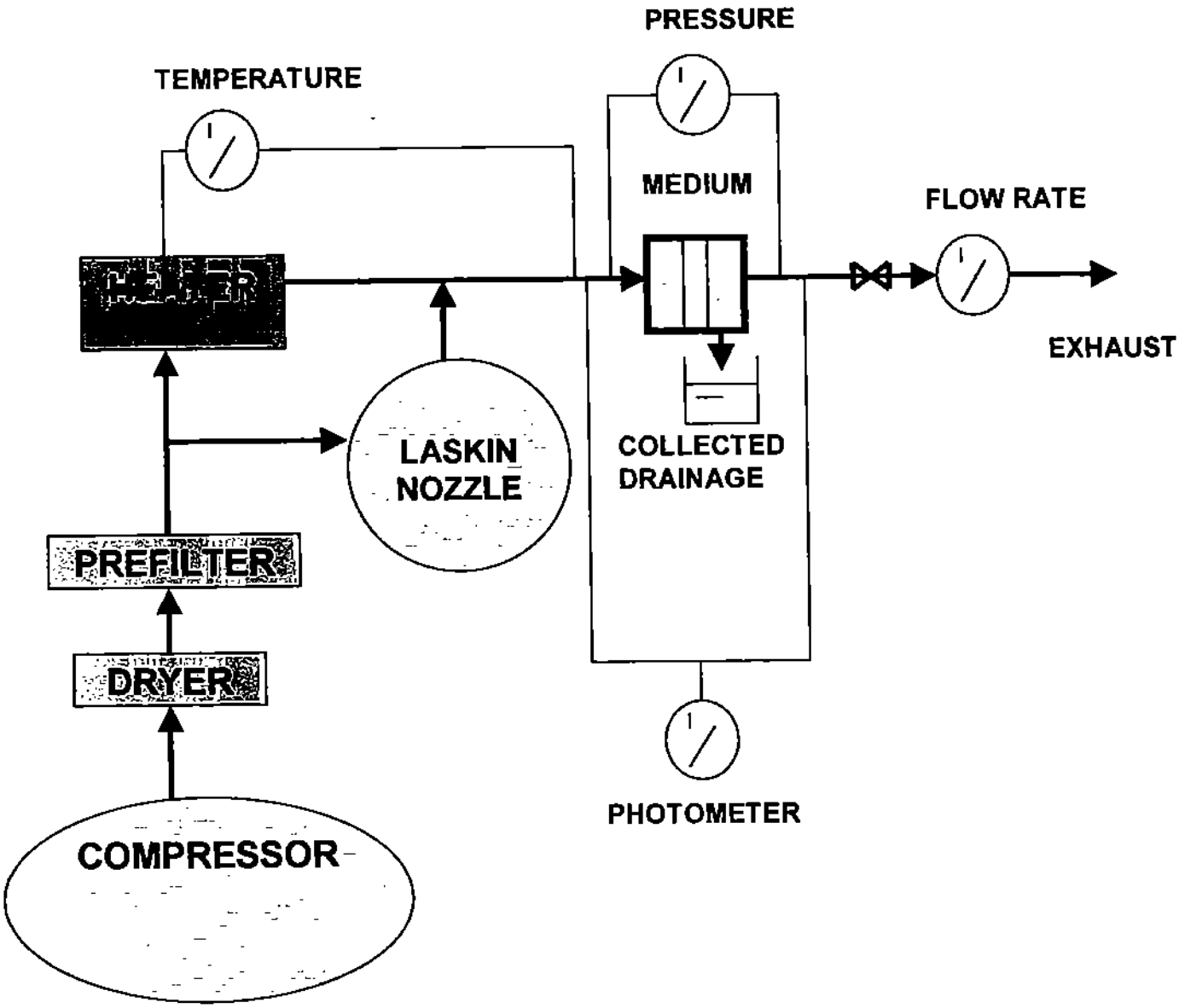

Figure 10. Diagram of the gas phase coalescence filtration experiment.

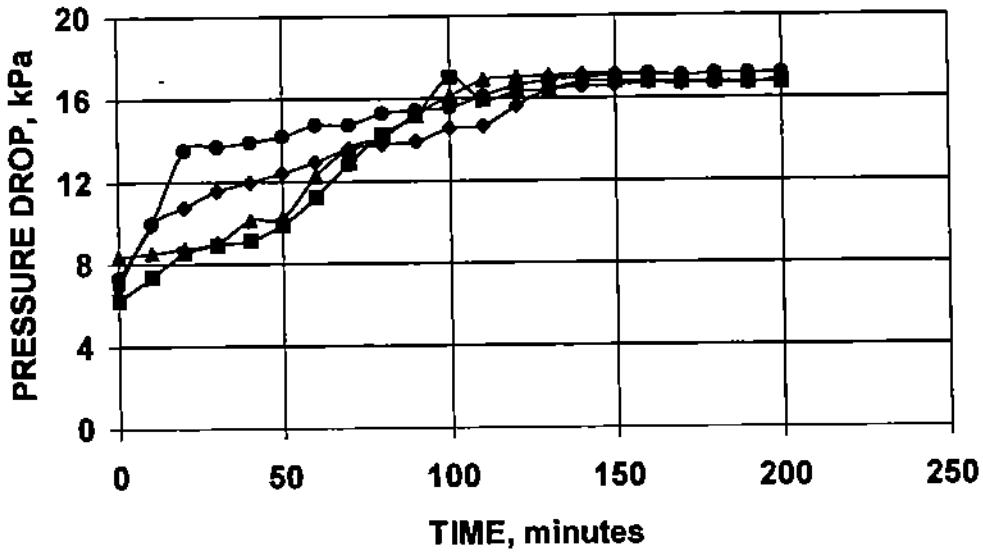

Figure 11. Pressure drop vs. time for glass fiber cakes with 0.07 grams of Nylon nanofiber. The multiple curves are for repetitions of experiments. The pressure drop across the medium levels off after about130 minutes indicating the filter is approaching steady state.

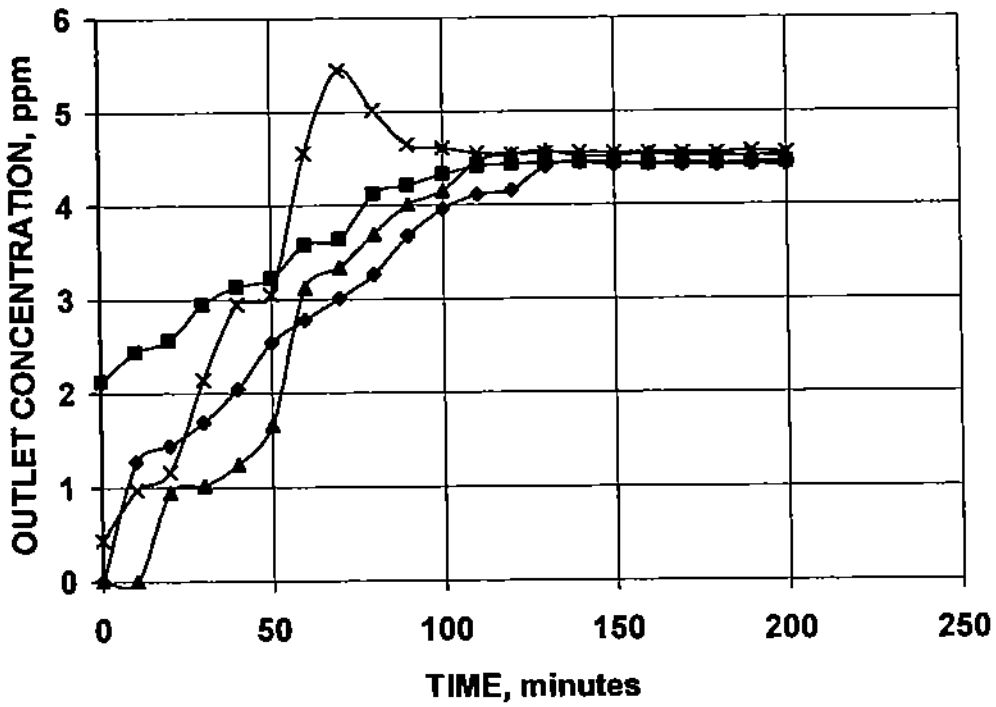

Figure 12. Outlet concentration versus time for glass fiber media with 0.07 g of Nylon nanofibers. Each curve represents a different experimental run to verify reproducibility.

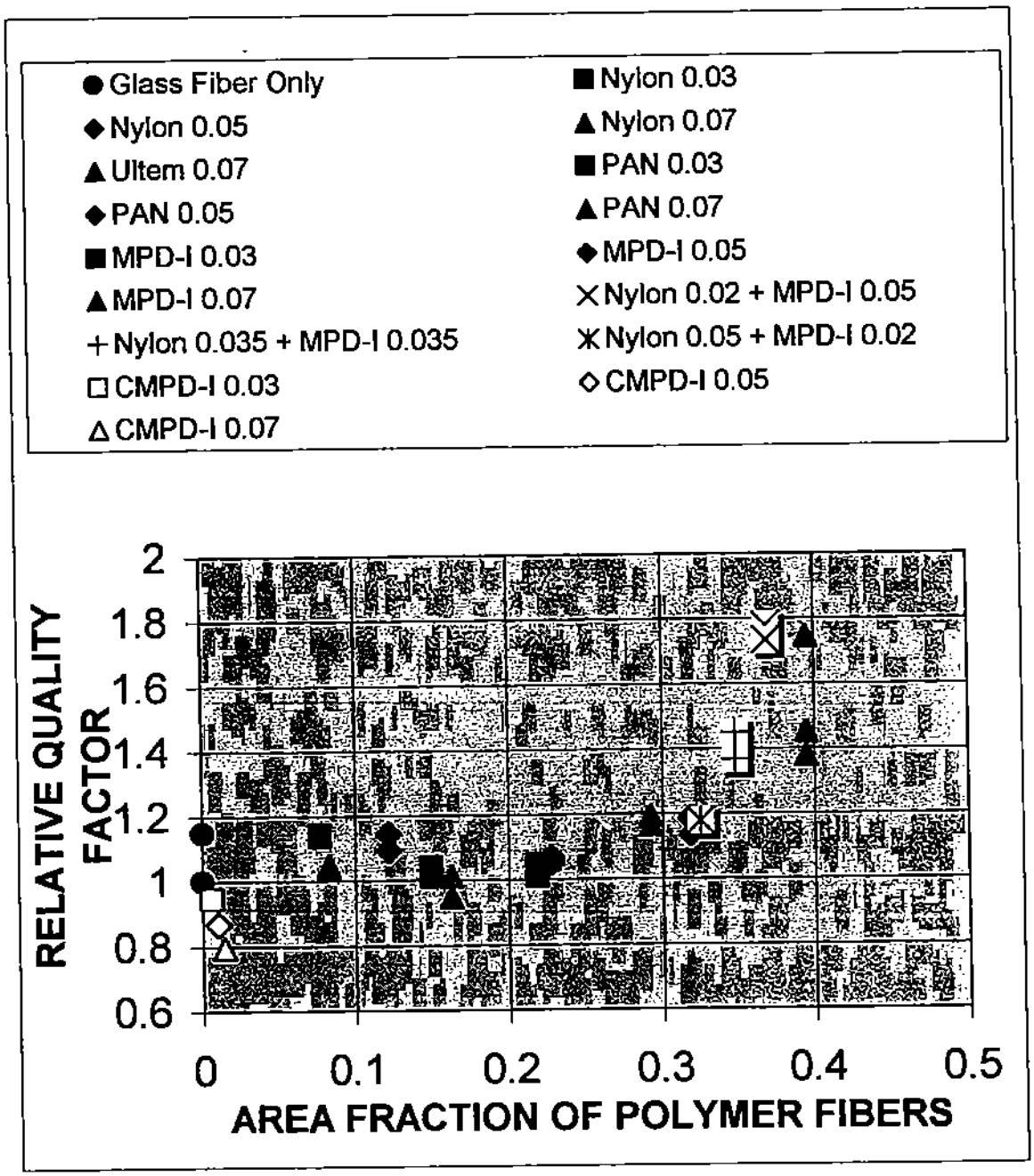

Figure 13. Plot of Relative Quality Factor versus the surface area fraction provided by nanofibers. The relative quality factor is defined as the quality factor divided by the quality factor of a glass fiber only medium. The nanofibers do not have much affect until they contribute more than about 25% of the surface area. The numbers in the legend indicate the number of grams of each polymer nanofiber added to two grams of glass fiber in the filter medium. CMPD-I stands for Conventional MPD-I Fiber as listed in Table 2.

Table 1. List of polymer types and typical solvents for electrospinning.

Polymer Class	Polymer type	Solvent
High performance polymers	Polyimides Polyamic Acid Polyetherimide	Phenol m-cresol Methylene chloride
Liquid crystalline polymers	Polyaramid Poly-gamma-benyzyl-glumate	Sulphuric acid Dimethylformamide
Co-polymers	Poly(p-phenylene Terephtalamide) Nylon6-polyimide	Sulphuric acid Formic acid
Textile Fiber Polymers	Polyacrylonitrile Polyethylene-terephtalate Nylon	Dimethylformamide Trifluoroacetic acid Dichloromethane
Electrically conductive polymers	Polyaniline	Sulphuric acid
Bio-Polymers	DNA Polyhyroxybutrate-valeate	Water chloroform

Table 2. Fibers and their average diameters used in the experiments.

FIBERS		DENSITY g/cm^3	AVERAGE DIAMETER nm	AREA PER MASS m^2/g
CONVENTIONAL MICROFIBERS	GLASS	2.2	1500	1.212
	MPD-I	1.18	7000	0.484
NANOFIBERS	MPD-I	1.18	150	22.6
	Nylon 6	1.12	250	14.3
	Polyacrylonitrile (PAN)	1.184	500	6.76
	Ultem 1000	1.28	1000	3.13